

TRANSIENT FAST DEFLAGRATION MODES  
IN METHANE–AIR MIXTURES**A. A. Borisov<sup>1,2</sup>, S. M. Frolov<sup>1,2,3</sup>, A. S. Koval<sup>1,2,3</sup>,  
A. E. Maikov<sup>1</sup>, and V. A. Smetanyuk<sup>1,2</sup>**<sup>1</sup>Center for Pulse-Detonation Combustion  
Moscow, Russia<sup>2</sup>N. N. Semenov Institute of Chemical Physics  
Russian Academy of Sciences  
Moscow, Russia<sup>3</sup>National Research Nuclear University  
“Moscow Engineering Physics Institute” (NRNU MEPhI)  
Moscow, Russia

Experiments show that the combined effect of acceleration of the flow due to the passage of the combustion wave from a larger-diameter tube into a smaller-diameter tube and through turbulizing obstacles significantly reduces the run-up distance of the strong shock wave–reaction zone complex in a stoichiometric methane–air mixture: such a complex can be formed in a tube with turbulizing obstacles within a distance of  $\sim 1$  m ( $\sim 14$  diameters of the test section) from the ignition source and can propagate in such a tube at a velocity of 1300–1400 m/s. After the passage of the shock wave – reaction zone complex from the tube portion with turbulizing obstacles into the smooth portion, it propagates there at a velocity of 850–900 m/s, without substantial attenuation, at least over a distance of 0.5–1 m.

**Introduction**

Methane, the main component of natural gas, is a combustible gas most commonly used in practice. Methane–air mixtures may be formed in a variety of conditions, in both confined and unconfined spaces. The explosibility of such mixtures has been investigated for several hundred

years. Although detonation in methane–air mixtures is very difficult to initiate due to the low reactivity of methane in reactions with air oxygen, a detonative explosion is traditionally considered the most dangerous and destructive.

At present, it is generally accepted that the smallest diameter of a smooth tube in which the detonation of a methane–air mixture can be initiated under normal conditions (for example, by a detonation wave propagating from an oxygen-based mixture, an active charge explosion, or by the gasdynamic focusing of a relatively weak shock wave) is 80–100 mm (see, e. g., [1–3]), although there is evidence [4] on the possibility of direct initiation of detonation (likely overdriven detonation) in a tube of diameter 50 mm. The critical energy of direct detonation initiation in methane–air mixtures in tubes reaches 50–70 g of high explosive [2,5] or 9–10 MJ/m<sup>2</sup> [4,6].

Today, it can be only assumed that the detonability limits of methane–air mixtures in tubes for a strong initiation and deflagration-to-detonation transition (DDT) are close to each other because the published data on DDT in tubes with methane–air mixtures are very contradictory. For example, according to the estimates made in [2,7], the DDT run-up distance for a stoichiometric methane–air mixture in a smooth tube should reach 50–125 tube diameters; however, today, there is neither experimental evidence supporting these estimates, nor facts about the very possibility of DDT in smooth tubes. The availability of regular obstacles inside the tube shortens the DDT run-up distance to 20–30 tube diameters [8–17]. However, according to [9,10], under normal conditions, the limiting tube diameter reduces to 50 mm [9], or even to 36 mm [10], whereas according to [12,14], it remains the same for direct detonation initiation (100 mm [12], or ~94 mm [14]), while according to [13], it increases (the authors of [13] reported that in a 121-millimeter-diameter tube with regular annular turbulizing obstacles, DDT in a stoichiometric methane–air mixture is possible only at initial pressures above 2 atm). In all these cases, it is assumed that detonation wave formed as a result of DDT can propagate in a self-sustained mode in a smooth section attached to the tube's section with turbulizing obstacles. Note that, in contrast to [9,10,13], where regular annular turbulizing obstacles or a Shchelkin spiral were used, in [12], special patented turbulizing obstacles were employed, whereas in [14], specially profiled turbulizing obstacles were used to ensure an

optimal harmonization of the rates of flame acceleration and strengthening of the shock wave generated by the flame, so as to provide conditions for “fast DDT” (according to the terminology of [18]).

Along with detonation, there are fast deflagration modes of combustion. Of greatest interest from the point of view of explosion safety are modes of combustion of methane–air mixtures with the formation of intense pressure waves capable of producing significant destruction. Such modes are transient between flame propagation at apparent velocities of several tens of meters per second and normal detonation propagating at velocities of 1600–1800 m/s. The transient combustion modes include so-called galloping detonation [1], for which detonation regions alternate with regions where the shock wave and the flame front are separated, as well as nonideal detonation in rough tubes and tubes with regular obstacles [19–22], for which the flame and shock wave are sufficiently closely connected with each other only at the periphery of the tube due to the self-ignition of the mixture in areas of reflection of the shock wave from roughness elements or obstacles. In the literature, all these modes are referred to by one term: fast deflagration combustion. When studying such destructive combustion modes, it is important not only to assess the possibility of their occurrence, but also to identify the conditions under which they arise within short distances from the ignition source. The latter is important for assessing the risks of accidents and for designing the equipment for explosion hazard predictions. In addition, it is important for the practical use of transient combustion regimes in various technological devices [23], for example, in new-type pulse-detonation burners, which provide a combined impact on objects: shock-wave (mechanical) and thermal [14, 16].

The aim of this paper is to determine the conditions under which fast deflagration modes with intense shock waves, similar to the detonation mode, can arise as a result of mixture ignition with a source that does not generate initial shock waves. For this purpose, the present authors specially selected such geometric parameters of the tube that are not best for DDT, namely: (*i*) the tube diameter was 70 mm, which provided [1] a steady propagation of detonation in a 17-meter-long smooth tube only in stoichiometric methane–air mixture, and even so with noticeable wave velocity fluctuations; and (*ii*) the length of the section over which the development of the process was recorded did not exceed 2.5 m.

## Experimental Setup

The rapid development of turbulence in the gas stream ahead of the flame is known to be one of the major factors that accelerate flame propagation and, hence, the formation of an intense pressure wave. There are two ways of intensification of turbulence in the flow: to place turbulizing obstacles [8] and to increase the gas flow velocity [14–16]. While the first method is widely used in studies of DDT [9–22], the second one has received less attention. In most practical situations, the gas mixture is initially at rest, so that a high flow velocity can arise only in the course of the combustion process itself due to the expansion of the reaction products. In reality, combustion can arise in a large volume and then move on to other volumes through channels where the flow ahead of the flame accelerates dramatically.

In the present work, both approaches to accelerating the combustion process have been used: by creating an initial turbulent gas flow and by making the flame to become turbulized on obstacles. Figure 1a shows a schematic diagram of the experimental setup. It consists of three interconnected sections: a precombustion chamber (*A*), booster (*B*) and test section (*C*) with turbulizing obstacles. The precombustion chamber is intended for reliable ignition of the mixture in the booster; the booster serves to create an initial turbulent gas flow in the test section; the turbulizing obstacles in the test section additionally turbulize the flame and create hot spots as shock waves are reflected.

In most experiments, the precombustion chamber was a tube 51 mm in inner diameter and 180 mm in length (its volume was 0.37 l). Near the closed end of the precombustion chamber, a spark ignition source was placed, whereas its open end communicated with the booster through a flow-restricting washer with a circular central hole of diameter 16 mm. In what follows, these experiments will be referred to as experiments without activation. In some experiments, the precombustion chamber was a tube with internal diameter of 12.7 mm and a length of 800 mm (with a volume of 0.1 l) with two closed ends. One end accommodated an ignition source in the form of an electrically fused wire, whereas the other had six 3-millimeter-diameter radial holes evenly spaced over the perimeter of the tube cross section. The portion of the tube with holes was slightly deepened into the booster via an adapter. The experiments

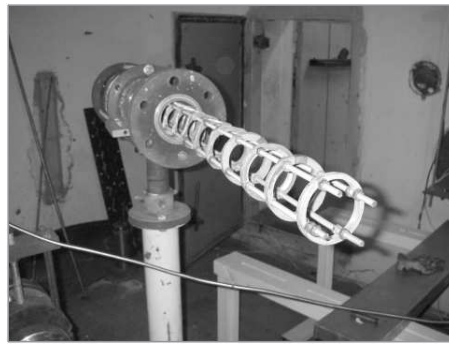
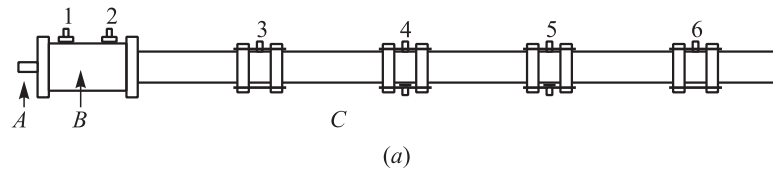


**Figure 1** Schematic diagram of the experimental setup (a) and photograph of turbulizing obstacles (b)

with such a precombustion chamber will be referred to as experiments with activation.

In the experiments without activation, the precombustion chamber, booster, and test section were filled with a stoichiometric methane–air mixture. The experiments with activation were performed to investigate how the ignition energy and power influence the development of the explosive process: the precombustion chamber was filled with a stoichiometric methane–oxygen mixture; the amount of mixture introduced, determined from the pressure drop in 1-liter bottle, did not exceed 0.1 l. In all cases, the methane–air mixture in the booster was ignited by one or more turbulent jets of combustion products outflowing from the precombustion chamber through the flow-restricting washer or the radial holes.

The booster was a straight tube 130 mm in diameter and 280 mm in length, one end of which communicated with the precombustion chamber, while the other with the test section. To speed up the combustion

of the mixture, a partition with twelve 14-millimeter-diameter holes evenly spaced along its perimeter was placed in the booster. In some experiments, the booster was additionally equipped with a second partition (downstream of the first) with 8 holes of diameter 14 mm.

The test section was a straight tube with a diameter of 70 mm and a length of 2.5 m, one end of which communicated with the booster, whereas the other was open to atmosphere. The open end of the test section enabled to introduce in it a 0.5- to 1.5-meter-long assembly of identical turbulizing obstacles (Fig. 1*b*). A single turbulizing obstacle was a ring with external and internal diameters of 70 and 50 mm, respectively, and a thickness of 4 mm. The flow blockage ratio of such a ring equals 0.49. In some experiments, a ring aperture with a blockage ratio of 0.67 was placed.

Stoichiometric methane–air mixture was prepared manometrically in a large-volume (30 l) mixer equipped with a fan for forced mixing at a pressure up to 3 atm. In experiments without activation, the mixture was introduced through the precombustion chamber, with the amount of mixture flushed through the setup before ignition being not less than the 8 to 9-fold volume of the setup. In experiments with activation, a 0.1-liter methane–oxygen mixture portion was injected into the precombustion chamber immediately before ignition.

The data-acquisition system included two low-frequency and four high-frequency pressure sensors and two photodiodes. Low-frequency pressure sensors 1 and 2 (see Fig. 1*a*) were installed in the booster, whereas high-frequency sensors 3–6 in the test section. Photodiodes L1 and L2 were mounted in the same sections as the high-pressure sensors. The signals from the pressure sensors and photodiodes were fed into a personal computer via an analog-to-digital converter. The pressure sensor signals were used to measure the velocity of propagation of arising pressure waves (the maximum relative error was estimated as 5%, with allowance for the possible blurring of the front). The pressure sensors were not pressure-calibrated; so, the analysis was based only on the measured velocities of the wave fronts. The signals from the photodiodes made it possible to determine the position of the light emission front relative to the wave front, as well as the average speed of propagation and the characteristic width of the emission front (relative error in determining the front velocity was 10% taking into account the field of view of the photodiode).

In the experiments, the energy and power of the ignition pulse in the precombustion chamber (with and without ignition activation), the number of perforated partitions in the booster (experiments with one and two partitions), the configuration of the test section (experiments with different location of turbulizing obstacles), and the configuration of the joint between the booster and test section (with and without the ring aperture) have been varied.

## Experimental Results and Discussion

For convenience of presenting the experimental results, Table 1 shows the location of the pressure sensors and photodiodes in these experiments (the distance to the sensor/photodiode was measured from the inner wall of the booster from the side of the precombustion chamber). In all the reported experiments, the first turbulizing obstacle in the test section was located at a distance of 610 mm from the beginning of the booster and the portion of the test section from the booster to the first turbulizing obstacle was smooth.

The purpose of experimental series I was to determine the structure of the pressure waves in the obstructed section at activated ignition. Figure 2 shows the pressure waveform (recorded by sensors 3–6) and emission signals (recorded by photodiodes L1 and L2) in one of the experiments of this series. The mean velocity of the primary shock wave within the smooth portion of the test section is  $\sim 450\text{--}500$  m/s. The signal from pressure sensor 4 located inside the assembly of turbulizing obstacles shows a sharp increase of pressure in the primary shock wave caused by the merger with an intense secondary wave. The amplitude of the formed shock wave is approximately an order of magnitude greater than the amplitude of the primary shock wave within the smooth por-

**Table 1** Location of pressure sensors and photodiodes (in mm)

Run series	Pressure sensor						Photodiode	
	1	2	3	4	5	6	L1	L2
I	20	260	613	945	1277	1617	945	1277
II	20	613	945	1277	1617	1982	1277	1617
III	20	260	613	945	1277	1617	945	1277

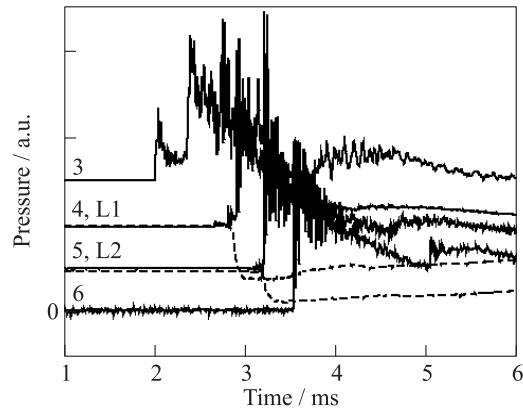


**Figure 2** Pressure profiles recorded by sensors 3–6 (solid curves) and luminescence intensity profiles recorded by photodiodes L1 and L2 (dashed curves) in experiment of series I

tion of the test section. Such a wave can arise only when a significant amount of mixture locally explodes. The cause of the explosion can be either the rapid combustion of a strongly turbulized mixture near obstacles after the arrival of the flame or the self-ignition of local mixture volumes during multiple reflections of the shock wave from obstacles. In the authors' opinion, the fact that the front of the shock wave (pressure signals 4 and 5 in Fig. 2) virtually coincides with the luminescence front (signals L1 and L2) provides more evidence in favor of the second mechanism: the local self-ignition of the mixture at multiple reflections of the shock wave from obstacles. In other words, the shock wave – reaction zone complex propagates here by the mechanism of detonation in rough tubes [19–22].

Analysis of pressure waveforms in Fig. 2 shows that in the region of turbulizing obstacles, this complex accelerates to  $\sim 1000$  m/s. Remind that in this series of experiments, the primary shock wave was initiated by using a small amount of methane–oxygen mixture supplied to the precombustion chamber. The question arises whether explosive processes such as that shown in Fig. 2 are possible in the ignition of a stoichiometric methane–air mixture without activation. To answer this question, consider the results of experimental series II.

In series II, the setup was purged before ignition with a stoichiometric methane–air mixture, but in contrast to experiments of series I, a 0.37-liter precombustion chamber was used but methane–oxygen mixture was not introduced in it. Another difference between the conditions of series II from those of series I is the presence of a second perforated partition in the booster, designed for intensifying mixture combustion. Figure 3*a* shows pressure profiles (recorded by sensors 1–6) and luminescence emission profiles (recorded by photodiodes L1 and L2) in one of the experiments of series II. It can be seen that in this experiment, an intense shock wave arises at the very beginning of the test-section portion with turbulizing obstacles (sensor 3) and within this area (between sensors 3 and 4) its speed reaches  $\sim 1400$  m/s (!). The time of arrival of the shock wave at sensor 4 almost coincides with the beginning of deflection of the signal of photodiode L4, located in the same cross section of the tube; i.e., the shock wave–reaction zone complex propagates here by the mechanism of detonation in rough tubes, involving local self-ignitions of the mixture as a result of multiple reflections of the shock wave from obstacles. After the shock wave leaves the tube portion with turbulizing obstacles and enters the smooth portion of the test section, its propagation velocity rapidly decreases to 850–900 m/s and then remains approximately constant. Such a decrease in the wave velocity is caused by a change in the conditions under which the chemical reactions behind the shock front occur: within the smooth portion of the test section, no local self-ignitions of the mixture at multiple reflections of the shock wave from obstacles occur.

Interestingly, the time of arrival of the shock wave at sensor 5 also almost coincides with the deflection of the luminescence signal of photodiode L1, located in the same cross section in the smooth portion of the tube. In the authors' opinion, the reason for which the shock wave–reaction zone complex continues to propagate by the mechanism of detonation in rough tubes is associated with a significant heterogeneity of the flow in the smooth tube after the shock wave leaves the portion of the tube obstructed with turbulizing obstacles. The rapid spontaneous self-ignition of the mixture behind the shock front at the wall of the tube could be caused by ongoing reflections of transverse shock waves, which inevitably make the wave front essentially non-one-dimensional.

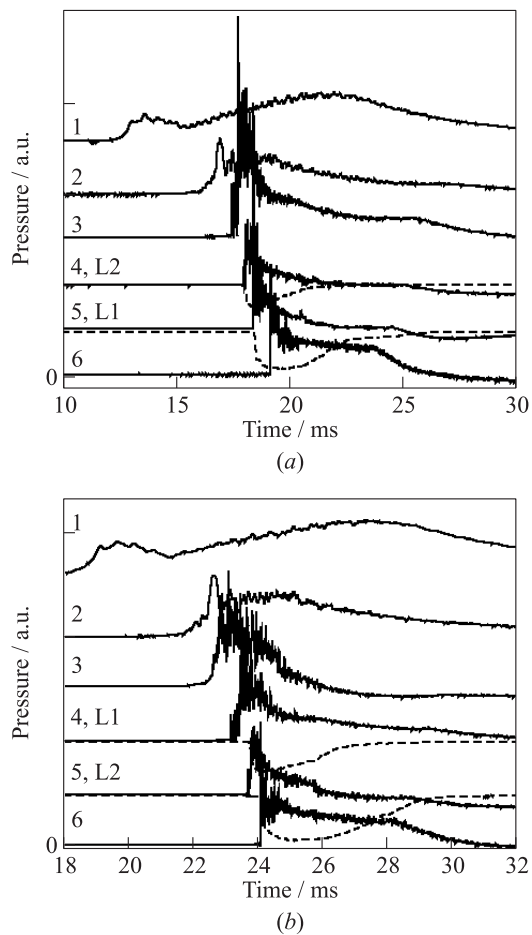


**Figure 3** Pressure profiles recorded by sensors 1–6 (solid curves) and luminescence intensity profiles recorded by photodiodes L1 and L2 (dashed curves) in experiments of series II (a) and III (b)

Thus, the high-velocity shock wave–reaction zone complex can arise and propagate in a stoichiometric methane–air mixture even without activating the ignition with a small amount of methane–oxygen mixture. Such a complex in experimental series II was produced only

by increasing the rate of combustion of the mixture in the booster by placing an additional perforated partition.

In experiments of series III, a ring aperture was set between the booster and the test section to reduce the flow cross section by 67%, all other conditions being the same as in series II. The objective of series III was to study the effect of the linear velocity of gas outflow from the booster (and, hence, the level of turbulization of the fresh mixture in the test section) on the dynamics of the formation of the shock wave–reaction zone high-velocity complex.

The result of one of the experiments in series III is presented in Fig. 3*b*. In contrast to series II, in the experiments of series III, a shock wave with a relatively gradual pressure rise enters the tube portion with turbulizing obstacles, not a shock wave with a sharp front as in Fig. 3*a*. Nevertheless, within the tube portion with turbulizing obstacles, this wave transforms into a shock wave and propagates at a velocity of  $\sim 1300$  m/s. Interestingly, in contrast to experiments of series II, in the experiments of series III, the luminescence front (signal from photodiode L1 in Fig. 3*b*) at the location of pressure sensor 4 lags behind the leading shock wave by  $\sim 500$   $\mu$ s. This means that in the shock wave–reaction zone high-speed complex, the mechanism of propagation of the reaction zone apparently changes: it propagates due to the rapid combustion of strongly turbulized volumes of fresh mixture near obstacles as they encounter the propagating turbulent flame. As in series II, in the experiments of series III, the velocity of the shock wave after it reaches the smooth portion of the test section decreased from  $\sim 1300$  to 850–900 m/s. In this case, the time lag of the reaction zone (signal from photodiode L2 in Fig. 3*b*) behind the shock wave (pressure sensor signal in Fig. 3*b*) remains at a level of 500  $\mu$ s.

The results of experimental series III indicate that an increase of the flow velocity and turbulence intensity in the fresh mixture facilitates the establishment of hazardous modes of combustion of methane mixtures.

## Concluding Remarks

Thus, the experiments performed show that the combined effect of acceleration of the flow due to the passage of the combustion wave from a larger-diameter tube (booster) into a smaller-diameter tube (test sec-

tion) and through turbulizing obstacles significantly reduces the run-up distance of the strong shock wave–reaction zone complex in a stoichiometric methane–air mixture: such a complex can be formed in a tube with turbulizing obstacles within a distance of  $\sim 1$  m ( $\sim 14$  diameters of the test section) from the ignition source and can propagate in such a tube at a velocity of 1300–1400 m/s. After the passage of the shock wave – reaction zone complex from the tube portion with turbulizing obstacles into the smooth portion, it propagates there at a velocity of 850–900 m/s, without substantial attenuation, at least over a distance of 0.5–1 m. Note that in the experiments with tubes of constant diameter 174 and 520 mm equipped with regular turbulizing obstacles [11], the shock-wave propagation velocity of 1300–1400 m/s was achieved within distances of 40 and 30 diameters, respectively, which is 2–3 times higher than in the present authors’ experiments. Experiments [2] with the passage of normal gas detonation into a constant-diameter tube with Shchelkin spiral showed that in such a tube, the shock wave–reaction zone complex propagates at a velocity not higher than 1000 m/s. All this suggests that transient combustion processes in systems composed of connecting channels of different diameters and containing portions with turbulizing obstacles can be more dangerous and destructive than combustion in obstructed constant-diameter tubes.

## Acknowledgments

This work was supported by Russian Science Foundation (grant No. 14-13-00082).

## References

1. Borisov, A. A., and S. A. Loban’. 1977. Detonation limits of hydrocarbon–air mixtures in tubes. *Fiz. Goreniya Vzryva* 13(5):729-733.
2. Knystautas, R., C. Guirao, J. H. Lee, and A. Sulmistras. 1984. Measurement of cell size in hydrocarbon–air mixtures and predictions of critical tube diameter, critical initiation energy and detonation limits. In: *Dynamics of shock Waves, explosions and detonations*. Eds. Bowen, Manson, Oppenheim, and Soloukhin. Progress in astronautics and aeronautics ser. 94:23.

3. Frolov, S. M., V. S. Aksenov, and A. A. Skripnik. 2011. Detonation initiation in a natural gas-air mixture in a tube with a focusing nozzle. *Dokl. Phys. Chem.* 436:10–14.
4. Wolanski, P., C. W. Kauman, M. Sichel, and J. A. Nicholls. 1981. Detonation of methane-air mixtures. *Proc. Combust. Inst.* 18:1651–1616.
5. Kogarko, S. M. 1958. Detonation of methane-air mixtures and detonation limits for hydrocarbon-air mixtures in large diameter tube. *Sov. Tech. Phys.* 38(9):2072–2083.
6. Borisov, A. A. 1999. Initiation of detonation in gases and two-phase mixtures. In: *Gaseous and heterogeneous detonations: Science to applications*. Eds. G. Roy, S. Frolov, K. Kailasanath, and N. Smirnov. Moscow: ENAS Publ. 3.
7. Bartknecht, W. 1981. *Explosion*. Berlin: Springer.
8. Shchelkin, K. I. 1949. *Rapid combustion and spin detonation gases*. Moscow: Voenizdat. [In Russian.]
9. Lindstedt, R. P., and H. J. Michels. 1989. Deflagration to detonation transitions and strong deflagrations in alkane and alkene air mixtures. *Combust. Flame* 76:169–181.
10. Matsui, H.. 2002. Detonation propagation limits in homogeneous and heterogeneous systems. *J. de Phys. IV*. Pr7-11–Pt7-17.
11. Kuznetsov, M., G. Ciccarelli, S. Dorofeev, *et al.* 2002. DDT in methane-air mixtures. *Shock Waves* 12:215–220.
12. Vasil'ev, A. A. 2003. Optimization of accelerators of deflagration-to-detonation transition. In: *Confined detonations and pulse detonation engines*. Eds. G. Roy, S. Frolov, R. Santoro, and S. Tsyganov. Moscow: TORUS PRESS. 41–48.
13. Kuznetsov, M., V. Alekseev, I. Matsukov, and T. H. Kim. 2010. Ignition, flame acceleration and detonations of methane air mixtures at different pressures and temperatures. *8th ISHPMIE Proceedings*. Jokohama, Japan. Paper No. ISH\_118.
14. Frolov, S. M., V. S. Aksenov, V. S. Ivanov, S. N. Medvedev, V. A. Smetanyuk, K. A. Avdeev, and F. S. Frolov. 2011. Pulse-detonation burner unit operating on natural gas. *Russ. J. Phys. Chem. B* 5(4):625–627.
15. Frolov, S. M., V. S. Aksenov, K. A. Avdeev, A. A. Borisov, P. A. Gusev, V. S. Ivanov, A. S. Koval, S. N. Medvedev, V. A. Smetanyuk, F. S. Frolov, and I. O. Shamshin. 2013. Deflagration-to-detonation transition in a high-velocity flow with separate delivery of fuel and oxidizer. *Dokl. Phys. Chem.* 449(2):91–93.
16. Frolov, S. M., V. S. Aksenov, K. A. Avdeev, A. A. Borisov, V. S. Ivanov, A. S. Koval, S. N. Medvedev, V. A. Smetanyuk, F. S. Frolov, and

- I. O. Shamshin. 2013. Cyclic Deflagration-to-detonation transition in the flow-type combustion chamber of a pulse-detonation burner. *Russ. J. Phys. Chem. B* 7(2):137–141.
17. Zipf, R. K., V. N. Gamezo, M. J. Sapko, *et al.* 2013. Methane–air detonation experiments at NIOSH Lake Lynn Laboratory. *J. Loss Prevent. Proc. Ind.* 26:295–301.
18. Frolov, S. M. 2008. Fast deflagration-to-detonation transition. ISSN 1990-7931. *Russ. J. Phys. Chem. B* 2(3):442–455.
19. Lee, J. H. S., R. Knystautas, and A. Feiman. 1984. High speed turbulent deflagrations and transition to detonation in H<sub>2</sub>–air mixtures. *Combust. Flame* 56:227–239.
20. Zeldovich, Ya. B., A. A. Borisov, B. E. Gelfand, S. V. Khomik, and A. E. Maikov. 1984. Low-speed combustion modes kvazidetonnatsionnye fuel -air mixtures in rough tubes. *Dokl. Akad. Nauk SSSR* 279(6):1359.
21. Zeldovich, Ya. B., B. E. Gelfand, Ya. M. Kazhdan, and S. M. Frolov. 1986. Propagation of detonation in a rough pipe considering braking and heat. *Combustion Explosion* 3:103–112.
22. Gelfand, B. E., S. M. Frolov, and M. A. Nettleton. 1991. Gaseous detonations — a selective review. *Prog. Energy Combust. Sci.* 17(4):327–371.
23. Frolov, S. M. 2003. Prospects for the use of detonation combustion of fuels in the energy and transport. *Tyazhel. Mashinostroen.* [Heavy Machinery] 9:18–22. [In Russian.]
24. Gelfand, B. E., S. M. Frolov, and S. P. Medvedev. 1990. Measurement and calculation of the attenuation of hydrocarbons in a rough pipe. *Combustion Explosion* 26(3):91–95.